Chemistry & Biology, Vol. 10, 81–89, January, 2003, ©2003 Elsevier Science Ltd. All rights reserved. DOI 10.1016/S1074-5521(03)00002-4

Induction and Inhibition of *Pseudomonas aeruginosa* Quorum Sensing by Synthetic Autoinducer Analogs

Kristina M. Smith,[1] Yigong Bu,[2] and Hiroaki Suga[1,2,*]
[1]Department of Biological Sciences
[2]Department of Chemistry
University at Buffalo
State University of New York
Buffalo, New York 14260

Summary

We synthesized a library of *Pseudomonas aeruginosa* autoinducer analogs with variation targeted to the homoserine lactone (HSL) moiety and discovered a new agonist, 3-oxo-C_{12}-(2-aminocyclohexanol), capable of activating LasR as a transcription factor. We reconstructed two sets of focused libraries against the quorum-sensing transcription factors LasR and RhlR, respectively. Opposing the prediction that both proteins should have the same binding site for HSL, it was surprising to find that these two related proteins respond to different structural motifs. This suggests that the HSL binding site differs in these proteins. We also found that subtle structural modifications to the agonists yielded compounds with antagonist activity. We performed a series of assays to show that inhibition of quorum sensing by these antagonists significantly reduced the production of virulence factors and biofilm formation.

Introduction

Pseudomonas aeruginosa is known to cause serious infections in certain immunocompromised individuals (reviewed in [1]). As one of the most frequent nosocomially acquired pathogens, it infects cancer patients receiving chemotherapy, burn patients, those on ventilators or with catheters, AIDS patients, and others. Most notably, it is the cause of mortality in nearly all individuals with cystic fibrosis (CF), the most common fatal genetic disorder in the U.S. [2]. Abnormalities in the lung tissue of CF patients allow *P. aeruginosa* colonization, causing prolonged inflammation, tissue damage, and eventually respiratory failure.

The unusually large *P. aeruginosa* genome [3] facilitates its adaptability to varied environments, and thus it is found ubiquitously and is nearly impossible to eliminate from hospital environments. Also encoded in its genome is a suite of virulence factors that contribute to pathogenicity, including secreted proteases, toxins, hemolysins, and an exopolysaccharide that composes biofilm [4–6]. Formation of biofilm, where cells attach to tissue and then secrete a slimy polysaccharide matrix to encase the bacterial community, is one of the most challenging problems in treating chronic *P. aeruginosa* infections [7]. Once this structure forms, the colony is protected from the patient's immune system and less susceptible to drug treatments.

P. aeruginosa uses a quorum-sensing (QS) mechanism of gene regulation to control expression of these virulence factors [6, 8–11]. First discovered in the marine photobacterium *Vibrio fischeri*, QS is a mechanism by which bacterial communities can communicate to rapidly alter gene expression based on cell population density [12]. Small amounts of a secreted signaling compound called an autoinducer (AI) accumulate with increasing population density (reviewed in [13]). These compounds pass between cells and, when present at concentrations representative of a "quorum," bind a regulatory protein, thereby activating it as a transcription factor. The regulatory protein is a member of the LuxR family of transcription factors, and targets for transcriptional activation include genes encoding the LuxR protein and the autoinducer synthase, a LuxI homolog. This creates a positive feedback, autoinducing loop.

The QS system in *P. aeruginosa* is controlled by two distinct yet interrelated pathways [14], the *las* and *rhl* systems. This organism possesses two LuxR type proteins, LasR and RhlR, and two LuxI type AI synthase proteins, LasI and RhlI. The AI compound produced by the I proteins is an N-acyl-homoserine lactone. Each I protein produces a compound with a unique acyl chain (reviewed in [15]), and each AI compound is sensed specifically by binding with high affinity to its cognate R protein. In *P. aeruginosa*, LasI synthesizes AI1 (3-oxo-C_{12} HSL) [16], which activates LasR. Similarly, RhlI synthesizes AI2 (C_4 HSL) [17], which activates RhlR. The LasR protein is the first to be activated, and it controls expression of the RhlR pathway via transcriptional activation of *rhlR* [18] and possibly *rhlI* [19], and putatively posttranslationally by binding of the LasI product (AI1) to the RhlR protein [18]. This prevents activation of RhlR by AI2 in the early stages of QS activation when AI2 concentrations are very low. In addition to inducing transcription of genes encoding QS proteins, LasR and RhlR each have numerous gene targets, most of which code for proteins involved in the disease process or necessary for survival within a host [6, 8, 14].

There now exists overwhelming evidence that QS is required for *P. aeruginosa* to cause disease [4, 9, 20–25]. Disruption of QS genes or elimination of specific QS-controlled virulence factors results in less severe, treatable infections. Since conventional antibiotic therapies lack the efficacy to deal with chronic *P. aeruginosa* infections, new targets for alternative therapies are needed. Because QS is required for pathogenicity, it is an ideal target for drug design [26–29]. The LasR protein is considered the "master regulator" of QS as activation of LasR by AI1 initiates the QS cascade. The LasR protein has been difficult to purify in an active form, and therefore its structure has not been determined. This means that neither a cell-free in vitro assay system for the discovery of antagonists nor knowledge for rational design of antagonists is available. Therefore, cell-based

*Correspondence: hsuga@buffalo.edu

screening of random analog libraries is the only available method to discover antagonists.

Previous work to isolate autoinducer antagonists focused on altering the side chain [26, 30]. These attempts provided evidence that the length of the side chain can be altered somewhat with little effect on activity, but drastic changes of length or substitution with bulky groups proximal to the HSL group eliminates activity. No potent antagonists were discovered from these studies. Since HSL is the common structural element in all AIs from LuxR/LuxI-type QS systems, it likely plays a critical role in inducing R protein activity. However, the structural elements of the HSL required for R protein activation have not been explored. Very few AI analogs with alterations at the HSL moiety have been synthesized and tested for biological activity. Among these, only substitution of HSL with homocysteine lactone exhibited a comparable activity to *P. aeruginosa* AI1 [30]. Clearly much work needs to be done before we have sufficient knowledge of the R protein-HSL interaction to design effective QS inhibitors.

Very recently, progress has been made on the path to elucidate the structure of R proteins. The crystal structure of TraR, the LuxR homolog from *Agrobacterium tumefaciens*, complexed with its AI and DNA, was published [31]. The crystal shows the HSL ring keto group in a hydrogen bond with Trp57. This residue as well as Asp70 and Tyr53, which interact with the amide group of the acyl-HSL linkage, are conserved in both LasR and RhlR. However, the AI binding site is not completely conserved between the published structure of TraR and either LasR or RhlR, and neither LasR nor RhlR is strongly activated by the *A. tumefaciens* AI, 3-oxo-C_8-HSL [30]. The variability in AI structure conferring R protein specificity is limited to the length and substitutions of the acyl side chain [11]. Does this suggest that all R proteins bind the HSL moiety in a similar manner? Can we modify the HSL structure in such a way as to create a general antagonist that can be applied to all R proteins simply by substituting the appropriate acyl chain? The answer to these questions will aid in the rational design of analogs that can bind and inhibit R proteins in organisms such as *P. aeruginosa* and others of medical and economic importance that use QS to regulate essential life processes.

To explore the above questions, we synthesized a library of AI1 analogs in which the 3-oxo-C_{12} side chain was retained and the HSL group was altered to various amines and alcohols (a total of 96 molecules were synthesized) (Y.B., K.M.S., and H.S., unpublished data). To screen our library for biological activity, we used a *P. aeruginosa* strain in which both AI synthase genes had been knocked out (PAO-JP2, *lasI*, *rhlI*) [14] harboring plasmid p*lasI*-LVAgfp [32]. When grown in the presence of exogenously added AI1, the LasR-AI1 complex activates transcription of the *lasI* promoter that controls *gfp* expression. This provides a simple, high-throughput method to detect the activity of analogs by measuring fluorescence. The compounds in the library were screened for their ability to activate expression of GFP. Several novel agonists were discovered, and this screening result is reported elsewhere (Y.B., K.M.S., and H.S., unpublished data).

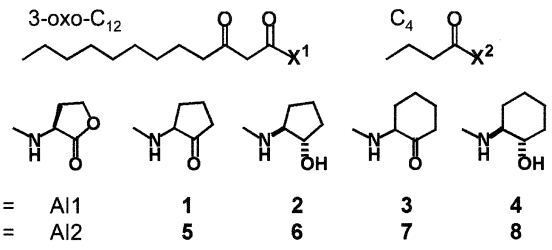

Figure 1. Chemical Structures of Autoinducers and Analogs

AI1, 3-oxo-C_{12}HSL; AI2, C_4 HSL; **1**, 3-oxo-C_{12}-(2-aminocyclopentanone); **2**, 3-oxo-C_{12}-(2-aminocyclopentanol); **3**, 3-oxo-C_{12}-(2-aminocyclohexanone); **4**, 3-oxo-C_{12}-(2-aminocyclohexanol); **5**, C_4-(2-aminocyclopentanone); **6**, C_4-(2-aminocyclopentanol); **7**, C_4-(2-aminocyclohexanone); **8**, C_4-(2-aminocyclohexanol).

To explore further the requirements for LasR binding and activation, we chose to focus on the most active compound, 3-oxo-C_{12}-(2-aminocyclohexanol) (Figure 1, **4**), which was able to induce GFP at concentrations comparable to the natural AI1 (Figures 2A and 2B, **4**). Superimposition of the amino and hydroxyl groups in this molecule with the amino and keto groups in HSL suggests similarities in structure. This led us to hypothesize that a 5- or 6-membered ring with a keto or hydroxl group (or other hydrogen bond acceptor) adjacent to the amine is sufficient for both binding and activation of LasR. To test this hypothesis, we synthesized the series of molecules shown in Figure 1 (compounds **1–3**). We were also interested in whether analogs binding to one R protein could bind other R proteins simply by substituting the cognate side chain. We therefore synthesized a second series of molecules (Figure 1, **5–8**) with C_4 side chains and tested their ability to activate RhlR using an *rhlI-gfp* reporter strain, PAO-JP2 (p*rhlI*-LVAgfp) [32].

Results and Discussion

Reporter Gene Assays

Using the PAO-JP2 (p*lasI*-LVAgfp) reporter strain, we first tested activity of the 3-oxo-C_{12} molecules, AI1 and **1–4**. Strong QS induction by AI1 was evidenced by the high GFP signal observed at as low as 1 μM of AI1 (Figures 2A and 2B, AI1). Our previously identified agonist, 3-oxo-C_{12}-(2-aminocyclohexanol) **4**, showed strong agonist activity with GFP induction only 2-fold less than AI1 at 1 μM and comparable to AI1 at higher concentrations (Figures 2A and 2B, **4**). 3-oxo-C_{12}-(2-aminocyclopentanone) **1** is structurally more similar to AI1 than **4**, since the oxygen of HSL was simply replaced with carbon in **1**. Hence, we expected that **1** would have strong agonist activity. Contrary to this prediction, **1** was able to induce the reporter only at a very high concentration (Figures 2A and 2B, **1**). Even more surprising, compounds **2** and **3** were nearly unable to induce the reporter, even at high concentrations (Figures 2A and 2B, **2** and **3**).

The C_4 compounds (A12 and **5–8**) were analyzed for agonist activity using PAO-JP2 (p*rhlI*-LVAgfp) (Figures 2C and 2D). Induction of GFP expression in this reporter requires addition of both AI1 and AI2. The AI2 control

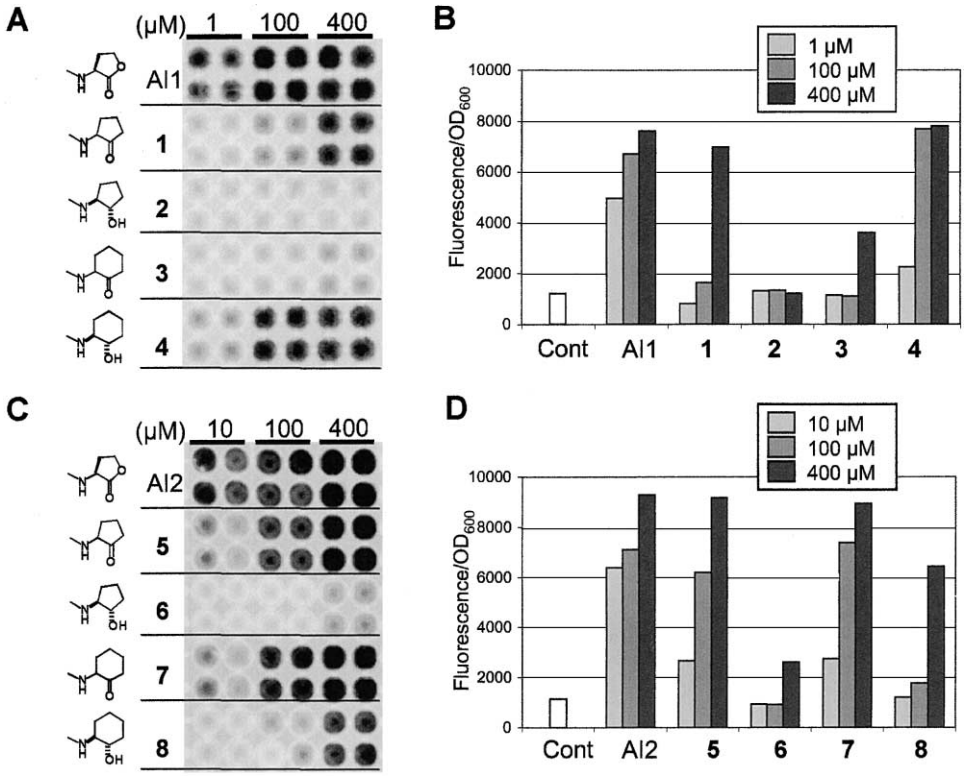

Figure 2. Reporter Gene Induction by Autoinducers and Their Analogs

(A) Molecular Imager scan of 96-well plate containing PAO-JP2 (p*lasI*-LVAgfp) in the presence of 1, 100, and 400 μM of the designated 3-oxo-C_{12} compound.

(B) Quantification of results of 3-oxo-C_{13} compounds. Cont, negative control of untreated cell (not shown in [A]). Average fluorescence of four replicate wells was corrected for cell density by dividing by OD_{600} of cell culture. The standard deviation was derived from three independent experiments shown in (A).

(C) Molecular Imager scan of 96-well plated containing PAO-JP2 (p*rhlI*-LVAgfp) in the presence of 1 μM AI1 and 10, 100, and 400 μM designated C_4 compound.

(D) Quantification of results of C_4 compounds. Data analysis was the same as (B).

and agonist assays, therefore, were performed in the presence of 1 μM AI1 and increasing concentrations of AI2 or analog (Figures 2C and 2D). Both ketone derivatives, **5** and **7**, showed strong agonist activity, inducing the reporter at just 10 μM (Figures 2C and 2D, **5** and **7**). In contrast, the 2-aminocyclopentanol derivative **6** had no agonist activity. Moreover, the 2-aminocyclohexanol derivative **8** had very little AI2 agonist activity; it could induce only moderate GFP expression at 400 μM (Figures 2C and 2D, column **8**).

As mentioned above, we initially assumed that since 2-aminocyclopentanone (**1** and **5**) and 2-aminocyclohexanone (**3** and **7**) have a keto group, they would better mimic the HSL structure than 2-aminocyclopentanol (**2** and **6**) and 2-aminocyclohexanol (**4** and **8**). In fact, in the *rhl* circuit, the ketone derivates are better agonists of AI2 than the alcohol derivatives. This is also consistent with the crystal structure of the TraR-3-oxo-C_8 HSL complex, which shows the ketone participating in an H bond. Presumably, an alcohol substitution could maintain the H bond, but less efficient binding would be expected. The results for the AI1 analogs, however, do not fit this pattern. In the *las* circuit, 2-aminocyclohexanol **4** is the strongest agonist, 2-aminocyclopentanone **1** is a weak agonist, and 2-aminocyclohexanone **3** has no agonist activity. Thus, based on our results, we propose that the microenvironment of the protein-HSL interface differs between LasR, RhlR, and TraR.

The most intriguing observation is that a subtle structural change from hydroxyl to keto group on the cyclohexane ring (**4** → **3**), or from keto to hydroxyl group on the cyclopentane ring (**1** → **2** or **5** → **6**), drastically reduced agonist activity. It is unlikely that such a small structural difference would completely eliminate binding to the respective R protein. A more likely, alternative explanation is that the cyclopentanol (**2**) and cyclohexanone (**3**) compounds can still bind LasR with similar affinity but are unable to activate it. Therefore, we speculated that compounds **2** and **3** might act as AI1 antagonists. Similarly, compound **6** should maintain the ability to bind RhlR and therefore might act as an AI2 antagonist.

Antagonist Assays

Based on the above hypothesis, we performed a competition assay of **2** and **3** against AI1, using strain PAO-JP2 (p*lasI*-LVAgfp). As predicted, compound **2** inhibited GFP expression approximately 70% at a 100-fold excess concentration over AI1 (Figure 3A), and compound **3**

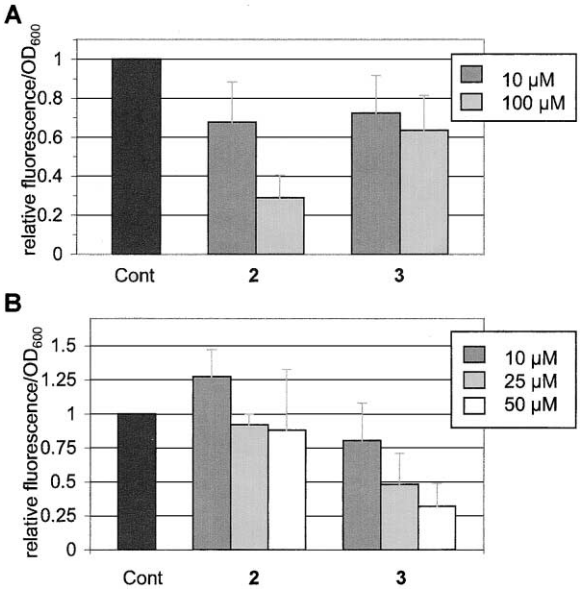

Figure 3. Antagonist Assays

(A) GFP expression by PAO-JP2 (p*lasI*-LVAgfp) in the presence of 1 μM AI1 alone (control, black bar) or 1 μM AI1 plus **2** or **3**.

(B) GFP expression by PAO-JP2 (p*rhlI*-LVAgfp) in the presence of 1 μM AI1 and 10 μM AI2 (control, black bar) or 1 μM AI1 and 10 μM AI2 plus **2** or **3**.

had a lesser inhibitory effect (35% reduction) under the same conditions. It should be noted that this inhibition experiment was performed with competition against **1** μM AI1, a concentration typically produced by wild-type *P. aeruginosa* [17]. These results suggest that both molecules bind LasR and prevent it from being activated by AI1. This view is supported by the compounds' inability to inhibit GFP expression when the *lasI* promoter is replaced with a *lac* promoter in strain PAO-JP2 (pTdK-GFP) [32] (data not shown). It should also be noted that cell growth was not affected by the addition of **2** or **3** at concentrations up to 400 μM (data not shown). Thus, it appears that compounds **2** and **3** act as specific inhibitors of QS-controlled promoters. Compound **6** was also tested for its ability to compete against AI2, but no inhibition of the *rhlI-gfp* reporter gene was seen (data not shown).

Next, we tested the ability of **2** and **3** to inhibit the *rhlI-gfp* reporter strain PAO-JP2 (p*rhlI*-LVAgfp), since this expression is also AI1 dependent. The Iglewski group recently reported that the *rhlI* promoter is induced primarily by the LasR-AI1 complex [19], but we see no induction of this promoter with the addition of only AI1 (data not shown). It is possible that the *rhlI-lacZ* reporter used in their study is more sensitive than the *rhlI-gfp* construct used in our study, and the small amount of GFP induced by AI1 is below our limit of detection. However, since both AI1 and AI2 are required to induce GFP from the PAO-JP2 (p*rhlI*-LVAgfp) reporter, we interpret our data in the context of earlier experiments that showed predominantly RhlR-AI2 activation of the *rhlI* promoter [33]. Surprisingly, compound **2** showed no antagonist activity in this assay (Figure 3B). More promising results were obtained from the assay of compound **3**, where GFP expression of the *rhlI-gfp* reporter was inhibited by greater than 60% at 50 μM when competing against 1 μM AI1 and 10 μM AI2 (Figure 3B).

Inhibition by compound **3** of the *rhlI-gfp* reporter was greater than that seen with the *lasI-gfp* reporter. Results from the *lasI-gfp* assay suggest that **3** inhibits LasR-AI1-dependent activation of transcription (Figure 3A). Since the *rhlR* promoter is also activated by LasR-AI1, inhibition of *rhlI-gfp* in the presence of **3** is likely due to inhibition of LasR-AI1-dependent activation of *rhlR* expression. This then translates into reduced activation of RhlR-AI2-dependent *rhlI-gfp* expression. It is also possible, however, that **3** directly interacts with RhlR and prevents AI2 binding, since AI1 is able to act as an antagonist against RhlR and prevent binding by AI2 [18]. The AI2 analog with the same ring structure as compound **3** (compound **7**, 2-aminocyclohexanone) is a strong agonist of RhlR. This supports the speculation that **3** could enter the AI binding site of RhlR and antagonize the RhlR-AI2 interaction. The chain length of RhlR autoinducers appears to be the determining factor regulating RhlR activation, since C_4HSL activates RhlR but 3-oxo-C_{12}HSL antagonizes it, and no C_4 analogs have been identified that can antagonize it. Regardless of the mechanism of inhibition by compound **3**, since the *rhlI* target is further downstream in the LasR signaling pathway than *lasI*, we would expect to see stronger inhibition of *rhlI* than *lasI*.

Virulence Factor Assays

In order to provide further evidence that compounds **2** and **3** are disrupting QS, we tested their ability to reduce expression of virulence factors in both the AI synthase knockout (PAO-JP2) and wild-type (PAO1) *P. aeruginosa* strains. We chose to assay two important virulence factors in *Pseudomonas* infections: first, the pigment pyocyanin that is required for disease in the *Arabidopsis thaliana* [34], *Caenorhabditis elegans* [4], and *Galleria mellonella* [35] infection models and causes serious tissue damage in chronic lung infections [36]; second, the metalloprotease elastase B, which degrades immune components and causes tissue damage [37].

Strong induction of pyocyanin in *P. aeruginosa* PAO-JP2 requires addition of both AI1 and AI2 (Figures 4A and 4B). When compound **3** was added in combination with exogenous AIs, there was nearly complete inhibition of pyocyanin expression (Figures 4A and 4B). A very similar inhibitory effect by **3** was observed when wild-type *P. aeruginosa* (PAO1) was assayed (Figure 4C). The concentration-dependent inhibitory effect of **3** leads us to believe that **3** is specifically competing against AI activation of pyocyanin expression. Compound **2**, on the other hand, reduced pyocyanin expression by 50% in PAO-JP2 (Figures 4A and 4B), but the inhibition was not concentration dependent over the range tested. Moreover, **2** had no significant effect on PAO1 (Figure 4C). We therefore think that the inhibitory effect of **2** on pyocyanin expression is not as significant as that of **3**.

For the elastase B assay, a colorimetric assay was conducted using elastin congo red substrate, so the observed protease activity is predominantly due to elas-

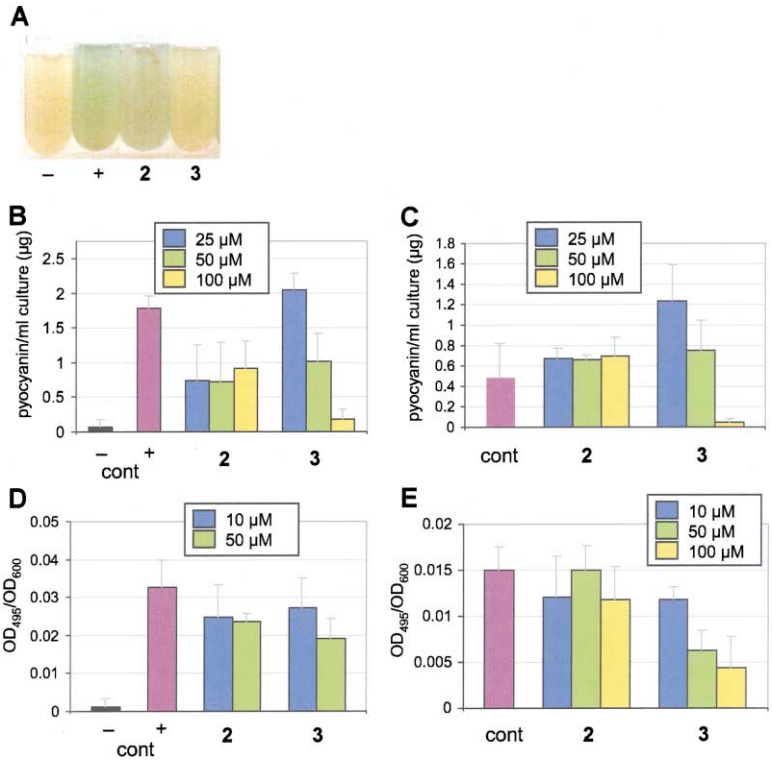

Figure 4. Virulence Factor Assays

(A) Pyocyanin expression by PAO-JP2. −, negative control; +, positive control, 25 μM each of AI1 and AI2; **2**, 25 μM each of AI1 and AI2 in the presence of 100 μM **2**; **3**, 25 μM each of AI1 and AI2 in the presence of 100 μM **3**.

(B) Quantification of pyocyanin expression by PAO-JP2 in the presence of various concentrations of **2** or **3**. −, negative control containing no AIs (black bar); +, positive control containing 25 μM each of AI1 and AI2 (purple bar); **2**, 25 μM each of AI1 and AI2 in the presence of **2**; **3**, 25 μM each of AI1 and AI2 in the presence of **3**.

(C) Quantification of pyocyanin expression of wild-type strain PAO1. The conditions are the same as (B), except for control (purple bar) where no AIs were added.

(D) Elastase B activity produced by PAO-JP2 in the absence (negative control, black bar) or presence of 5 μM AI1 and 10 μM AI2 (positive control, purple bar) or 5 μM AI1 and 10 μM AI2 plus **2** or **3**.

(E) Elastase B activity produced by PAO1 control (purple bar) or in the presence of **2** or **3**.

tase B and not other proteases that might be present in culture supernatants (Figures 4D and 4E) [38]. Our control experiment showed that 5 μM AI1 and 10 μM AI2 were required for consistent induction of elastase B activity in PAO-JP2. At 50 μM **3**, elastase activity was reduced to 60% of the positive control level (Figure 4D). When the same assay was performed on wild-type *P. aeruginosa*, elastase activity was reduced to 30% of the control level in the presence of 100 μM **3** (Figure 4E). These results indicate that **3** likely inhibits elastase B expression, although the inhibition was not as strong as that observed for pyocyanin expression. On the other hand, compound **2** had no significant effect on elastase activity produced by either strain (Figures 4D and 4E). Since **2** showed weaker inhibition of pyocyanin and elastase production than **3**, future studies focused solely on **3**.

Static Biofilm Assay

There is evidence that the chronic nature of *P. aeruginosa* infections is due in part to biofilm growth [39, 40]. Biofilm is an attached colony of bacteria protected from biocide treatment and the host immune response by a secreted polysaccharide matrix [41]. Its development in *P. aeruginosa* is QS controlled, and disruption of QS has been shown to eliminate or reduce biofilm development [22, 25, 42]. Prevention of biofilm growth continues to be a challenge, since treatment of biofilm colonies has proven extremely difficult.

We tested compound **3** for its effect on biofilm development in a 24 hr assay that looks at the early stages of biofilm formation. The static biofilm assay is a simple yet reliable method to monitor QS-controlled steps of biofilm formation [32]. Strain PAO-JP2 (pTdK-GFP) [32] contains a constitutively expressed GFP construct for visualization by scanning confocal laser microscopy. The PAO-JP2 autoinducer synthase knockout strain did not form a biofilm unless AIs were added (Figure 5A). When this strain was grown in the presence of AIs plus **3**, biofilm formation was completely inhibited (Figure 5A, right panel). Inhibition of biofilm formation in the wild-type strain PAO1 (pTdK-GFP) (Figure 5B) was less obvious, but there was a noticeable difference in biofilm morphology when grown in the presence of **3**. The above results provide additional evidence that compound **3** interferes with QS signaling and reduces the production of important virulence factors.

Conclusions and Outlook

The initial screen of our library yielded a potent agonist of AI1, and we elaborated this compound further to support our hypothesis that the HSL ring could be agonized by a 5- or 6-membered ring system with a hydrogen bond acceptor at position 1 (hydroxyl or oxo group). We targeted both the *las* and *rhl* systems in this study, synthesizing the same compounds with either a 3-oxo-C_{12} side chain or a C_4 side chain. The results of the study of agonist activity of the analogs were unexpected. We found that the requirements for binding of AI differ between the homologs LasR and RhlR. LasR was activated best by 3-oxo-C_{12}-(2-aminocyclohexanol), and RhlR was activated equally well by C_4-(2-aminocyclopentanone) and C_4-(2-aminocyclohexanone). Our results suggest that even though all I proteins synthesize an acylated HSL, the R proteins do not necessarily recognize the HSL moiety in the same manner. Further elaboration of

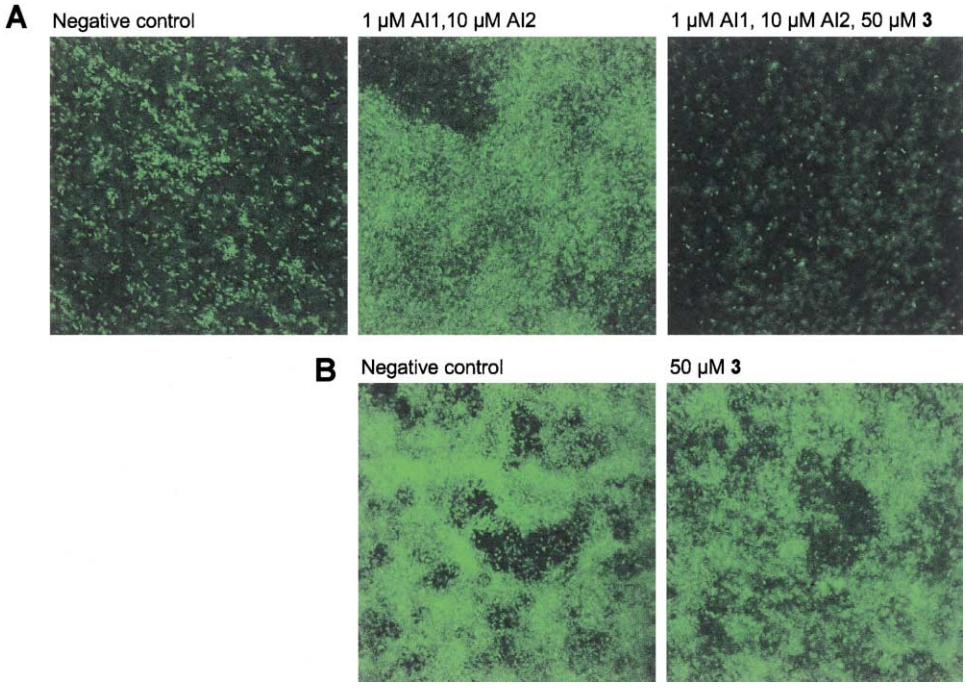

Figure 5. Static Biofilm Assay

(A) PAO-JP2 (pTdK-GFP) biofilm development in the presence of designated compounds.

(B) PAO-1 (pTdK-GFP) biofilm development in the absence (negative control) or presence of 50 μM **3**.

the structure of these synthetic agonists may provide new insights into the specificity of the R protein-AI interaction.

While attempting to elucidate structural elements required for agonist activity, we found compounds with antagonist activity. Compound **2**, 3-oxo-C_{12}-(2-aminocyclopentanol), inhibited the *lasI-gfp* reporter very effectively but had no effect on the *rhlI-gfp* reporter and was only mildly effective at disrupting QS-regulated virulence factor expression. Why did compound **2** fail to exhibit inhibitory action in the *rhlI-gfp* reporter and virulence factor assays? Our current hypothesis relates to the issue raised in the discussion that **3** may directly bind RhlR and prevent AI2 binding. Compound **2** may be unable to interact with RhlR, so its QS inhibitory activity is mediated purely through disruption of the LasR-AI1 interaction. This speculation is supported by the fact that the AI2 analog with the same ring structure as **2** (compound **6**, 2-aminocyclopentanol) does not activate RhlR. The AI binding site of RhlR, therefore, cannot accommodate a cyclopentanol ring (**2** or **6**), but can accommodate a cyclohexanone ring (**3** and **7**). These questions require further study.

Compound **3**, 3-oxo-C_{12}-(2-aminocyclohexanone), inhibited both the *lasI* and *rhlI* reporters, pyocyanin, elastase, and biofilm. While **3** appears to inhibit the *rhl* cascade somewhat, it was disappointing that none of the AI2 analogs showed antagonist activity toward the *rhl* cascade. AI1 has weak antagonist activity toward RhlR [18], as might **3**, following the general trend that long chain AIs antagonize R proteins that are activated by short chain AIs [26]. We currently lack a potent antagonist for the *rhl* cascade, particularly one that does not agonize the *las* cascade. Future studies will focus on discovery of a specific AI2 antagonist that could be used in combination with our AI1 antagonist or a single compound capable of inhibiting both LasR and RhlR. It is necessary to discover such antagonists since both cascades need to be eliminated for effective QS inhibition, as there is evidence that the *rhl* cascade can become activated in the absence of the *las* cascade under certain selective conditions [43].

The most active *P. aeruginosa* AI1 antagonist previously identified, recently reported by Hentzer et al. [27], is derived from the halogenated furanones of *Delissea pulchra*. This compound displays similar properties to our compound **3** in that it inhibits QS at roughly 100-fold excess concentrations over the natural AIs. It is difficult to make direct comparisons of the activity of these compounds, however, since different promoters were used to control the reporter systems that determined activity. It should be noted that Whiteley et al. grouped QS promoters into four classes based on their responsiveness to AI1 versus AI2, and the degree and timing of that response [6]. Class I promoters, which include the *lasI* promoter used in our reporter assay, are induced early after a quorum is reached and respond strongly to only AI1. The *lasB* promoter used in the Hentzer study is a class IV promoter that requires both AI1 and AI2 for full induction and responds very little to AI1 alone. Perhaps this is not relevant when inhibition assays are performed in heterologous systems lacking other regulators of QS-controlled genes, but we should cautiously consider this when comparing data collected in *P. aeruginosa*. We think our system using a class I promoter is more difficult to inhibit, so our antagonist

may be more active than the Hentzer antagonist. Additionally, we saw inhibition of QS at physiologically relevant AI concentrations, where both natural AIs were at or above 1 μM [17]. Indeed, the concentrations used in our studies were much higher than those typically used in similar inhibition studies. It should also be noted that a primary advantage to our antagonist is the ease of synthesis of new analogs. The 3-oxo-C_{12}-(2-aminocyclohexanone) structure can easily be manipulated to generate new focused libraries to screen for stronger antagonists, and these analogs are expected to have lower toxicity than the halogenated analogs of *D. pulchra*.

Significance

The transcription factors of bacterial QS systems are important targets for efforts toward biocontrol strategies. We identified new agonists of both *P. aeruginosa* AIs that shed light on the unique R protein-AI interaction in each cognate pair. Compounds 1 and 4 activate LasR, while 5 and 7 activate RhlR. The observed variation in the active HSL analog structures between the 3-oxo-C_{12} and the C_4 derivatives clearly suggests that the microenvironment of the HSL binding site in these R proteins is different. We also discovered a moderately active AI1 antagonist (2) and a strong AI1 antagonist (3) that inhibits the QS cascade, resulting in reduced expression of important virulence factors and biofilm. Future studies will be conducted to test the effect of compound 3 on pathogenicity in a model host system. Most importantly, the discovered structural elements that exhibit antagonist activity will lead us to rational design of more focused libraries, and the knowledge gained from such investigations will aid in the discovery of potent inhibitors of QS.

Experimental Procedures

Synthesis of Autoinducer Analogs

N-*(*trans-*2-hydroxycyclopentyl)-3-oxododecanamide (2)*

To a solution of 3,3-ethylenedioxydodecanoic acid (55 mg, 0.213 mmol) [16] (Y.B., K.M.S., and H.S., unpublished data) and *trans*-2-amino-cyclopentanol hydrochloride (35 mg, 0.256 mmol, purchased from Aldrich, 52,586-3) in anhydrous DMF (2 ml) was added successively EDC (49 mg, 0.256 mmol), DMAP (32 mg, 0.256 mmol), and i-Pr_2NEt (45 μl, 0.256 mmol) at room temperature. The mixture was stirred for 18 hr. After removing DMF in vacuo, the residue was dissolved into ethyl acetate (20 ml) and washed with 0.1 M HCl saturated with NaCl (20 ml). The aqueous phase was extracted with ethyl acetate (3 × 40 ml). The combined organic extracts were dried over $MgSO_4$ and concentrated to give a crude intermediate (57 mg, 79%). The 3,3-ethylenedioxy protective group was deprotected by treatment of the intermediate dissolved in 1 ml CH_2Cl_2 with 1 ml 95% TFA for 2 hr at room temperature. The organic solvent was briefly removed under reduced pressure, and the residue was mixed with saturated aqueous $NaHCO_3$ followed by extraction with ethyl acetate (3 × 40 ml). The organic layers were combined and washed once with brine and dried over $MgSO_4$. After concentration, the residue was purified by flash chromatography on silica gel to give *N*-(*trans*-2-hydroxycyclopentyl)-3-oxododecanamide in the ketone form (14.8 mg, 0.050 mmol, R_f = 0.42) and the enol form (19.2 mg, 0.065 mmol, R_f = 0.15) in a total of 54% yield. Ketone form: IR (KBr) 3270, 2921, 1716, 1646, 1613, 1561 cm^{-1}; ^{1}H NMR (500 MHz, $CDCl_3$) δ 0.88 (t, *J* = 7 Hz, 3H), 1.20–1.35 (m, 12H), 1.48–1.52 (m, 1H), 1.58 (m, 2H), 1.60–1.78 (m, 2H), 1.81 (m, 1H), 2.05 (m, 1H), 2.16 (m, 1H), 2.52 (t, *J* = 7 Hz, 2H), 3.42 (s, 2H), 3.84 (m, 1H), 3.98 (m, 1H), 4.24 (s, 1H), 7.40 (s, 1H); ^{13}C (125 MHz, $CDCl_3$): 14.1, 21.3, 22.6, 23.3, 28.95, 29.20, 29.30, 29.35, 30.3, 31.8, 32.6, 44.0, 47.9, 60.7, 79.5, 167.5, 207.4; EI-HRMS calcd for $C_{17}H_{31}O_3N$ (M^+) 297.2298, found 297.2299. Enol form: IR (KBr) 2918, 2952, 1655, 1424, 1365, 832 cm^{-1}; ^{1}H NMR (500 MHz, $CDCl_3$) δ 0.88 (t, *J* = 7.5 Hz, 3H), 1.20–1.38 (m, 12H), 1.52 (m, 2H), 1.62 (m, 1H), 1.78–1.96 (m, 3H), 2.15 (td, *J* = 7 Hz, 1.5 Hz, 2H), 2.30 (m, 2H), 3.56 (m, 1H), 4.27 (m, 1H), 5.03 (d, *J* = 1.5 Hz, 1H), 6.82 (s, 1H); ^{13}C (125 MHz, $CDCl_3$) δ 14.1, 21.1, 22.6, 27.6, 28.9, 29.24, 29.29, 29.42, 30.66, 30.69, 31.8, 36.6, 57.3, 87.8, 98.2, 165.6, 168.7; EI-HRMS calcd for $C_{17}H_{29}O_2N$ (M-H_2O) 279.2193, found 279.2197.

N-*(*trans-*2-hydroxycyclohexyl)-3-oxododecanamide (4)*

The same procedure as the synthesis of **1** was performed, except that *trans*-2-amino-cyclohexanol hydrochloride was used instead of *trans*-2-amino-cyclopentanol hydrochloride. Column chromatography of the crude product gave **4** in the ketone form (23 mg, 0.074 mmol, R_f = 0.29) and enol form (11 mg, 0.035 mmol, R_f = 0.17) in a total of 51% yield. Ketone form: IR (KBr) 3274, 2927, 1715, 1652, 1617, 1564 cm^{-1}; ^{1}H NMR (500 MHz, $CDCl_3$) δ 0.88 (t, *J* = 7.5 Hz, 3H), 1.18–1.40 (m, 16H), 1.58 (m, 2H), 1.72 (m, 2H), 1.90–2.10 (m, 2H), 2.53 (t, *J* = 7.5, 2H), 3.35 (m, 1H), 3.43 (s, 2H), 3.67 (m, 1H), 7.19 (d, *J* = 5 Hz, 1H); ^{13}C (125 MHz, $CDCl_3$) δ 14.1, 22.6, 23.3, 23.9, 24.5, 28.9, 29.21, 29.31, 29.34, 31.2, 31.8, 34.2, 44.0, 48.3, 55.7, 75.2, 167.3, 207.5; EI-HRMS calcd for $C_{18}H_{33}O_3N$ (M^+) 311.2455, found 311.2463. Enol form: IR (KBr) 2921, 2853, 1668, 1452, 1040 cm^{-1}; ^{1}H NMR (500 MHz, $CDCl_3$) δ 0.88 (t, *J* = 7.5 Hz, 3H), 1.16–1.60 (m, 18H), 1.75 (m, 2H), 2.00–2.24 (m 4H), 3.25 (m, 1H), 3.84 (m, 1H), 5.02 (d, *J* = 2 Hz), 5.60 (s, 1H); ^{13}C (125 MHz, $CDCl_3$) δ 14.1, 22.7, 23.2, 23.4, 27.3, 28.9, 29.27, 29.33, 29.44, 31.5, 31.9, 32.2, 36.8, 54.2, 82.7, 97.4, 166.1, 167.8; EI-HRMS calcd for $C_{18}H_{31}O_2N$ (M-H_2O) 293.2349, found 293.2357.

N-*(2-oxocyclopentyl)-3-oxododecanamide (1)*

Oxalyl chloride (42.5 μl, 0.486 mmol) in 1 ml anhydrous CH_2Cl_2 was cooled to −78°C under an argon atmosphere, and anhydrous DMSO (69 μl, 0.974 mmol) was added via a syringe. The mixture was stirred for 2 min. **2** with the 3,3-ethylenedioxy protective group at the 2-oxo position (83 mg, 0.243 mmol) in 1 ml CH_2Cl_2 was added via a syringe, and the mixture was stirred for 15 min. To the resulting solution triethylamine (169 μl, 1.215 mmol) was added, and the stirring was continued for 5 min. After warming to room temperature, the reaction was quenched by the addition of 20 ml 0.1 M HCl. The resulting mixture was extracted with ethyl acetate (3 × 30 ml), and the combined organic layers were washed sequentially with saturated aqueous $NaHCO_3$ and brine. All the extracts were combined, dried ($MgSO_4$), and concentrated to give the crude intermediate **1** with the protective group (57 mg). This molecule was treated with 95% TFA in the same manner as in the synthesis of **2**, and its chromatographic purification on silica gel afforded **1** (42 mg, 0.14 mmol) in 85% yield. IR (KBr) 3244, 2927, 1752, 116, 1651, 1591, 1567 cm^{-1}; ^{1}H NMR (500 MHz, $CDCl_3$) δ 0.879 (t, *J* = 7.5 Hz, 3H), 1.20–1.36 (m, 12H), 1.52–1.64 (m, 2H), 1.64–1.76 (m, 1H), 1.80–1.92 (m, 1H), 2.04–2.16 (m, 1H), 1.98–2.08 (m, 1H), 2.36–2.44 (m, 1H), 2.53 (t, *J* = 7.5 Hz, 2H), 2.55–2.69 (m, 1H), 4.12–4.20 (m, 1H), 7.40 (d, *J* = 5 Hz, 2H); ^{13}C (125 MHz, $CDCl_3$) δ 14.0, 18.2, 22.6, 23.3, 28.92, 29.17, 29.28, 29.31, 29.61, 31.8, 35.0, 43.8, 48.4, 57.8, 166.0, 206.6, 214.5; EI-HRMS calcd for $C_{17}H_{29}O_3N$ (M^+) 295.2142, found 295.2145.

N-*(2-oxocyclohexyl)-3-oxododecanamide (3)*

The same procedure for the preparation of **1** was used, except that the starting material was **4** with the 3,3-ethylenedioxy protective group at the 2-oxo position (117 mg, 0.38 mmol). The crude product was purified by flash chromatography (hexane/EtOAc 1:2, R_f = 0.38) to give **3** (87 mg, 0.28 mmol) in 73% yield. IR (KBr) 3280, 2935, 1712, 1654, 1628, 1550 cm^{-1}; ^{1}H NMR (500 MHz, $CDCl_3$) δ 0.877 (t, *J* = 7 Hz, 3H), 1.20–1.34 (m, 12H), 1.36–1.44 (m, 1H), 1.55–1.70 (m, 3H), 1.76–1.84 (m, 1H), 1.84–1.95 (m, 1H), 2.11–2.20 (m, 1H), 2.36–2.44 (m, 1H), 2.50–2.60 (m, 3H), 2.60–2.65 (m, 1H), 3.41 (s, 2H), 4.45–4.55 (m, 1H), 7.53 (d, *J* = 4 Hz, 1H); ^{13}C (125 MHz, $CDCl_3$) δ 14.0, 22.6, 23.3, 24.0, 27.9, 28.96, 29.20, 29.31, 29.34, 31.8, 35.1, 41.1, 43.7, 49.2, 58.2, 165.3, 206.0, 207.0; EI-HRMS calcd for $C_{18}H_{31}O_3N$ (M^+) 309.2298, found 309.2284.

N-*(*trans-*2-hydroxy)cyclopentylbutanamide (6) and* N-*(*trans-*2-hydroxy)cyclohexylbutanamide (8)*

The procedure for the preparation of C_4-HSL was used for this series of molecules. The EDC-mediated coupling of butyric acid and *trans*-

2-amino-cyclopentanol or *trans*-2-amino-cyclohexanol afforded **6** in 66% yield or **8** in 82% yield. **6**: IR (KBr) 3284, 2960, 1643, 1567, 1058 cm^{-1}; ^1H NMR (500 MHz, $CDCl_3$) δ 0.952 (t, J = 7.5 Hz, 3H), 1.40–1.50 (m, 1H), 1.60–1.74 (m, 4H), 1.75–1.82 (m, 1H), 1.96–2.08 (m, 1H), 2.08–2.18 (m, 1H), 2.19 (t, J = 7 Hz, 2H), 3.80–3.86 (m, 1H), 3.92–4.00 (m, 1H), 4.90 (s, 1H), 6.28 (s, 1H); ^{13}C (125 MHz, $CDCl_3$) δ 13.6, 19.0, 21.1, 30.0, 32.3, 38.0, 60.5, 79.5, 175.3; EI-HRMS calcd for $C_9H_{17}O_2N$ (M^+) 171.1254, found 171.1257. **8**: IR (KBr) 3294, 2930, 1638, 1567, 1086, 1072 cm^{-1}; ^1H NMR (500 MHz, $CDCl_3$): 0.952 (t, J = 7.5 Hz, 3H), 1.15–1.20 (m, 4H), 1.60–1.80 (m, 4H), 1.98 (m, 2H), 2.20 (t, J = 7.5, 2H), 3.30–3.34 (m, 1H), 3.54–3.60 (m, 1H), 4.20 (s, 1H), 6.30 (d, J = 7 Hz, 1H); ^{13}C (125 MHz, $CDCl_3$) δ 13.5, 19.1, 24.0, 24.4, 31.3, 34.3, 38.4, 55.6, 74.8, 174.9; EI-HRMS calcd for $C_{10}H_{19}O_2N$ (M^+) 185.1410, found 185.1410.

N-2-oxocyclopentylbutanamide (5) and N-2-oxocyclohexylbutanamide (7)

Swern oxidation, similar to the synthesis of **1**, was performed to afford **5** in 60% yield and **7** in 48% yield. **5**: IR (KBr) 3256, 2963, 1744, 1641, 1555 cm^{-1}; ^1H NMR (500 MHz, $CDCl_3$) δ 0.954 (t, J = 7.5 Hz, 3H), 1.56–1.70 (m, 3H), 1.82–1.94 (m, 1H), 2.02–2.10 (m, 1H), 2.18–2.26 (m, 3H), 2.38–2.44 (m, 1H), 2.60–2.68 (m, 1H), 4.10–4.20 (m, 1H), 6.00 (s, 1H); ^{13}C (125 MHz, $CDCl_3$) δ 13.6, 18.0, 18.9, 30.1, 34.9, 38.1, 173.3, 215.4 EI-HRMS calcd for $C_9H_{15}O_2N$ (M^+) 169.1097, found 169.1101. **7**: IR (KBr) 3295, 2943, 1719, 1643, 1552 cm^{-1}; ^1H NMR (500 MHz, $CDCl_3$) δ 0.95 (t, J = 7 Hz, 3H), 1.25–1.40 (m, 1H), 1.60–1.70 (m, 3H), 1.78–1.90 (m, 2H), 2.10–2.19 (m, 1H), 2.20 (t, J = 7 Hz, 2H), 2.36–2.44 (m, 1H), 2.50–2.55 (m, 1H), 2.64–2.72 (m, 1H), 4.40–4.60 (m, 1H), 6.42 (s, 1H); ^{13}C (125 MHz, $CDCl_3$) δ 13.7, 19.1, 24.0, 28.1, 35.6, 38.6, 41.2, 58.0, 172.7, 208.0; EI-HRMS calcd for $C_{10}H_{17}O_2N$ (M^+) 183.1254, found 183.1259.

Reporter Gene Assays

Reporter strains were grown overnight in LB plus 300 μg/ml carbenicillin at 37°C and diluted to an OD_{600} of 0.1. Following an incubation of 1 hr, 200 μl of cell culture was added to individual wells of a 96-well plate containing appropriate amount of test compound(s). Plates were incubated for 6 hr and then scanned for fluorescence emission with a Molecular Imager (488 nm excitation and 695 nm bandpass filter). Fluorescence was quantified with ImageQuant software.

Virulence Factor Assays

For pyocyanin assay, cells were grown overnight in LB then washed in fresh media and diluted to an OD_{600} of 0.05. This culture was grown for 3–4 hr to midlog phase (OD_{600} of 0.3–0.5) and then diluted to an OD_{600} of 0.05, and aliquoted to test tubes containing appropriate amount of test compound(s). Following 18 hr of growth, pyocyanin was extracted from filtered culture supernatants and quantified using standard methods [44]. For elastase B assay, cells were grown overnight in PTSB media (5% Peptone, 0.1% Tryptic Soy Broth) at 37°C, washed, and diluted to an OD_{600} of 0.05, grown to midlog phase, washed again, and resuspended to an OD_{600} of 0.05. The culture was then added to test tubes containing test compound(s) and grown for 6 hr. Elastase B activity was quantified by incubation of 100 μl of filtered culture supernatant with 5 mg Elastin Congo red substrate and 1 ml of 10 mM Tris (pH 7.2), 1 mM $CaCl_2$ for 6 hr at 37°C with agitation. Elastase B activity is represented by the OD_{495} of the enzyme assay following reaction quenching with EDTA and centrifugation to remove unreacted substrate, divided by the OD_{600} of the cell culture.

Static Biofilm Assay

Cells were grown in M9 media (47.7 mM $Na_2HP_4 \cdot 7H_2O$, 21.7 mM KH_2PO_4, 8.6 mM NaCl, 18.7 mM NH_4Cl, 0.5% casamino acids, 11.1 mM glucose, 1 mM $MgSO_4$) plus carbenicillin (300 μg/ml) overnight, washed and resuspended to an OD_{600} of 0.05, grown to midlog phase, diluted to an OD_{600} of 0.05, and added to sterile shell vials containing glass coverslips (ViroMed Laboratories, Minneapolis, MN) on which the test compounds had been applied. Cultures were grown at 37°C with shaking for 30 min, and then allowed to sit at 37°C for an additional 23.5 hr. Coverslips were then rinsed and placed on slides for visualization using an MRC1024 Laser Scanning Microscope (Bio-Rad) with a Nikon Fluor-60× oil emersion objective lens (NA = 1.4), 488 nm argon laser, and OG515 filter.

Acknowledgments

This work was supported by the Interdisciplinary Research and Creative Activities Fund, Office of the Vice President for Research, University at Buffalo, awarded to H.S. We thank Barbara Iglewski for generously providing strains PAO-JP2 and PAO1 and plasmids p*lasI*-LVAgfp, p*rhlI*-LVAgfp, and pTdK-GFP. We thank Dr. Haridas Pudavar and the Institute for Lasers, Photonics, and Biophotonics for assistance with microscopy.

Received: November 14, 2002
Revised: December 11, 2002
Accepted: December 12, 2002

References

1. Van Delden, C., and Iglewski, B.H. (1998). Cell-signaling and the pathogenesis of *Pseudomonas aeruginosa* infections. Emerg. Infect. Dis. *4*, 551–560.
2. Lyczak, J.B., Cannon, C.L., and Pier, G.B. (2002). Lung infections associated with cystic fibrosis. Clin. Microbiol. Rev. *15*, 1059–1067.
3. Stover, C.K., Pham, X.Q., Erwin, A.L., Mizoguchi, S.D., Warrener, P., Hickey, M.J., Brinkman, F.S., Hufnagle, W.O., Kowalik, D.J., Lagrou, M., et al. (2000). Complete genome sequence of Pseudomonas aeruginosa PAO1, an opportunistic pathogen. Nature *406*, 959–964.
4. Mahajan-Miklos, S., Tan, M., Rahme, L.G., and Ausubel, F.M. (1999). Molecular mechanisms of bacterial virulence elucidated using a *Pseudomonas aeruginosa-Caenorhabditis elegans* pathogenesis model. Cell *96*, 47–56.
5. Tan, M., Rahme, L.G., Sternberg, J.A., Tompkins, R.G., and Ausubel, F.M. (1999). *Pseudomonas aeruginosa* killing of *Caenorhabditis elegans* used to identify *P. aeruginosa* virulence factors. Proc. Natl. Acad. Sci. USA *96*, 2408–2413.
6. Whiteley, M., Lee, K.M., and Greenberg, E.P. (1999). Identification of genes controlled by quorum sensing in *Pseudomonas aeruginosa*. Proc. Natl. Acad. Sci. USA *96*, 13904–13909.
7. Costerton, J.W., Stewart, P.S., and Greenberg, E.P. (1999). Bacterial biofilms: a common cause of persistent infections. Science *284*, 1318–1322.
8. Passador, L., Cook, J.M., Gambello, M.J., Rust, L., and Iglewski, B.H. (1993). Expression of *Pseudomonas aeruginosa* virulence genes requires cell-to-cell communication. Science *260*, 1127–1130.
9. Pearson, J.P., Feldman, M., Iglewski, B.H., and Prince, A. (2000). *Pseudomonas aeruginosa* cell-to-cell signaling is required for virulence in a model of acute pulmonary infection. Infect. Immun. *68*, 4331–4334.
10. de Kievit, T.R., and Iglewski, B.H. (2000). Bacterial quorum sensing in pathogenic relationships. Infect. Immun. *68*, 4839–4849.
11. Miller, M.B., and Bassler, B.L. (2001). Quorum sensing in bacteria. Annu. Rev. Microbiol. *55*, 165–199.
12. Nealson, K.H., Platt, T., and Hastings, J.W. (1970). Cellular control of the synthesis and activity of the bacterial luminescent system. J. Bacteriol. *104*, 313–322.
13. Bassler, B.L. (2002). Small talk: cell-to-cell communication in bacteria. Cell *109*, 421–424.
14. Pearson, J.P., Pesci, E.C., and Iglewski, B.H. (1997). Roles of *Pseudomonas aeruginosa las* and *rhl* quorum-sensing systems in control of elastase and rhamnolipid biosynthesis genes. J. Bacteriol. *179*, 5756–5767.
15. Schauder, S., and Bassler, B.L. (2001). The languages of bacteria. Genes Dev. *15*, 1468–1480.
16. Pearson, J.P., Gray, K.M., Passador, L., Tucker, K.D., Eberhard, A., Iglewski, B.H., and Greenberg, E.P. (1994). Structure of the autoinducer required for expression of *Pseudomonas aeruginosa* virulence genes. Proc. Natl. Acad. Sci. USA *91*, 197–201.
17. Pearson, J.P., Passador, L., Iglewski, B.H., and Greenberg, E.P. (1995). A second N-acylhomoserine lactone signal produced

by *Pseudomonas aeruginosa*. Proc. Natl. Acad. Sci. USA *92*, 1490–1494.
18. Pesci, E.C., Pearson, J.P., Seed, P.C., and Iglewski, B.H. (1997). Regulation of *las* and *rhl* quorum sensing in *Pseudomonas aeruginosa*. J. Bacteriol. *179*, 3127–3132.
19. de Kievit, T.R., Kakai, Y., Register, J.K., Pesci, E.C., and Iglewski, B.H. (2002). Role of the *Pseudomonas aeruginosa las* and *rhl* quorum-sensing systems in *rhlI* regulation. FEMS Microbiol. Lett. *212*, 101–106.
20. Tang, H.B., DiMango, E., Bryan, R., Gambello, M., Iglewski, B.H., Goldberg, J.B., and Prince, A. (1996). Contribution of specific *Pseudomonas aeruginosa* virulence factors to pathogenesis of pneumonia in a neonatal mouse model of infection. Infect. Immun. *64*, 37–43.
21. Preston, M.J., Seed, P.C., Toder, D.S., Iglewski, B.H., Ohman, D.E., Gustin, J.K., Goldberg, J.B., and Pier, G.B. (1997). Contribution of proteases and LasR to the virulence of *Pseudomonas aeruginosa* during corneal infections. Infect. Immun. *65*, 3086–3090.
22. Davies, D.G., Parsek, M.R., Pearson, J.P., Iglewski, B.H., Costerton, J.W., and Greenberg, E.P. (1998). The involvement of cell-to-cell signals in the development of a bacterial biofilm. Science *280*, 295–298.
23. Rumbaugh, K.P., Griswold, J.A., Iglewski, B.H., and Hamood, A.N. (1999). Contribution of quorum sensing to the virulence of *Pseudomonas aeruginosa* in burn wound infections. Infect. Immun. *67*, 5854–5862.
24. Calfee, M.W., Coleman, J.P., and Pesci, E.C. (2001). Interference with *Pseudomonas* quinolone signal synthesis inhibits virulence factor expression by *Pseudomonas aeruginosa*. Proc. Natl. Acad. Sci. USA *98*, 11633–11637.
25. Wu, H., Song, Z., Givskov, M., Doring, G., Worlitzsh, D., Mathee, K., Rygaard, J., and Hoiby, N. (2001). *Pseudomonas aeruginosa* mutations in *lasI* and *rhlI* quorum sensing systems result in milder chronic lung infection. Microbiology *147*, 1105–1113.
26. Kline, T., Bowman, J., Iglewski, B.H., de Kievit, T., Kakai, Y., and Passador, L. (1999). Novel synthetic analogs of the *Pseudomonas* autoinducer. Bioorg. Med. Chem. Lett. *9*, 3447–3452.
27. Hentzer, M., Riedel, K., Rasmussen, T.B., Heydorn, A., Andersen, J.B., Parsek, M.R., Rice, S.A., Eberl, L., Molin, S., Hoiby, N., et al. (2002). Inhibition of quorum sensing in *Pseudmonas aeruginosa* biofilm bacteria by a halogenated furanone compound. Microbiology *148*, 87–102.
28. Olsen, J.A., Severinsen, R., Rasmussen, T.B., Hentzer, M., Givskov, M., and Nielsen, J. (2002). Synthesis of new 3- and 4-substituted analogues of acyl homoserine lactone quorum sensing autoinducers. Bioorg. Med. Chem. Lett. *12*, 325–328.
29. Reverchon, S., Chantegrel, B., Deshayes, C., Doutheau, A., and Cotte-Pattat, N. (2002). New synthetic analogues of *N*-acylhomoserine lactones as agonists or antagonists of transcriptional regulators involved in bacterial quorum sensing. Bioorg. Med. Chem. Lett. *12*, 1153–1157.
30. Passador, L., Tucker, K.D., Guertin, K.R., Journet, M.P., Kende, A.S., and Iglewski, B.H. (1996). Functional analysis of the *Pseudomonas aeruginosa* autoinducer PAI. J. Bacteriol. *178*, 5995–6000.
31. Zhang, R.G., Pappas, T., Brace, J.L., Miller, P.C., Oulmassov, T., Molyneaux, J.M., Anderson, J.C., Bashkin, J.K., Winans, S.C., and Joachimiak, A. (2002). Structure of a bacterial quorum-sensing transcription factor complexed with pheromone and DNA. Nature *417*, 971–974.
32. de Kievit, T.R., Gillis, R., Marx, S., Brown, C., and Iglewski, B.H. (2001). Quorum-sensing genes in *Pseudomonas aeruginosa* biofilms: their role and expression patterns. Appl. Environ. Microbiol. *67*, 1865–1873.
33. Latifi, A., Foglino, M., Tanaka, K., Williams, P., and Lazdunski, A. (1996). A hierarchical quorum-sensing cascade in *Pseudomonas aeruginosa* links the transcriptional activators LasR and RhlR (VsmR) to expression of the stationary-phase sigma factor RpoS. Mol. Microbiol. *21*, 1137–1146.
34. Rahme, L., Tan, M., Le, L., Wong, S.M., Tompkins, R.G., Calderwood, S.B., and Ausubel, F.M. (1997). Use of model plant hosts to identify *Pseudomonas aeruginosa* virulence factors. Proc. Natl. Acad. Sci. USA *94*, 13245–13250.
35. Jander, G., Rahme, L.G., and Ausubel, F.M. (2000). Positive correlation between virulence of *Pseudomonas aerugiosa* mutants in mice and insects. J. Bacteriol. *182*, 3843–3845.
36. Wilson, R., Sykes, D.A., Watson, D., Rutman, A., Taylor, G.W., and Cole, P.J. (1988). Measurement of *Pseudomonas aeruginosa* phenazine pigments in sputum and assessment of their contribution to sputum sol toxicity for respiratory epithelium. Infect. Immun. *56*, 2515–2517.
37. Kon, Y., Tsukada, H., Hasegawa, T., Igarashi, K., Wada, K., Suzuki, E., Arakkawa, M., and Gejyo, F. (1999). The role of *Pseudomonas aeruginosa* elastase as a potent inflammatory factor in a rat air pouch inflammation model. FEMS Immunol. Med. Microbiol. *25*, 313–321.
38. Caballero, A.R., Moreau, J.M., Engel, L.S., Marquart, M.E., Hill, J.M., and O'Callaghan, R.J. (2001). *Pseudomonas aeruginosa* protease IV enzyme assays and comparison to other *Pseudomonas* proteases. Anal. Biochem. *290*, 330–337.
39. Singh, P.K., Schaefer, A.L., Parsek, M.R., Moninger, T.O., Welsh, M.J., and Greenberg, E.P. (2000). Quorum-sensing signals indicate that cystic fibrosis lungs are infected with bacterial biofilms. Nature *407*, 762–764.
40. Drenkard, E., and Ausubel, F.M. (2002). *Pseudomonas* biofilm formation and antibiotic resistance are linked to phenotypic variation. Nature *416*, 740–743.
41. O'Toole, G., Kaplan, H.B., and Kolter, R. (2000). Biofilm formation as microbial development. Annu. Rev. Microbiol. *54*, 49–79.
42. Shirtliff, M.E., Mader, J.T., and Camper, A.K. (2002). Molecular interactions in biofilms. Chem. Biol. *9*, 859–871.
43. Van Delden, C., Pesci, E.C., Pearson, J.P., and Iglewski, B.H. (1998). Starvation selection restores elastase and rhamnolipid production in a *Pseudomonas aeruginosa* quorum-sensing mutant. Infect. Immun. *66*, 4499–4502.
44. Essar, D.W., Eberly, L., Hadero, A., and Crawford, I.P. (1990). Identification and characterization of genes for a second anthranilate synthase in *Pseudomonas aeruginosa*: interchangeability of the two anthranilate synthases and evolutionary implications. J. Bacteriol. *172*, 884–900.